Dynamic Isomer Shift in Charge-Ordering Manganite Y 0.5 Ca 0.5 MnO 3 : Mössbauer Spectroscopy Study

ARTICLE *in* THE JOURNAL OF PHYSICAL CHEMISTRY B · MARCH 2005

Impact Factor: 3.3 · DOI: 10.1021/jp0444823 · Source: PubMed

THE JOURNAL OF PHYSICAL CHEMISTRY B LETTERS

2005, *109,* 1656−1659
Published on Web 01/13/2005

Dynamic Isomer Shift in Charge-Ordering Manganite $Y_{0.5}Ca_{0.5}MnO_3$: Mössbauer Spectroscopy Study

H. W. Tian, W. T. Zheng,* B. Zheng, X. Wang, Q. B. Wen, T. Ding, and Z. D. Zhao

Department of Materials Science, Key Lab of Automobile Materials of MOE, and National Key Lab of Superhard Materials, Jilin University, Changchun 130012, People's Republic of China

Received: December 4, 2004; In Final Form: December 23, 2004

We report the Mössbauer spectroscopy study on Fe-doped charge-ordering manganite $Y_{0.5}Ca_{0.5}MnO_3$. The dynamic isomer shift is observed for charge-ordering manganite, and its origin may be due to strong Jahn−Teller distortions in $Y_{0.5}Ca_{0.5}MnO_3$, causing electron−phonon coupling. The evolution of Mössbauer spectroscopy as a function of temperature shows two different phases with significantly different quadrupole splitting values below the charge-ordering transition temperature. This confirms that there exist two different Mn sites (i.e., Mn^{3+} and Mn^{4+} ions), which can be identified by the microscopic method of Mössbauer spectroscopy.

Perovskite manganites with mixed manganese valence, $R_{1-x}A_xMnO_3$, where R is a trivalent rare earth ion such as La^{3+} and Y^{3+} and A is a divalent alkaline earth ion such as Ca^{2+} and Sr^{2+}, have attracted a great deal of attention due to the anomalously large negative "colossal" magnetoresistance (CMR) for $0.2 < x < 0.5$.[1−3] Understanding the behavior of these Mn-based materials is a challenge for both experimentalists and theorists. CMR and related properties essentially arise from the double-exchange mechanism of electron hopping between the Mn^{3+} ($t_{2g}^3 e_g^1$) and Mn^{4+} ($t_{2g}^3 e_g^0$) ions, but this mechanism alone is insufficient to quantitatively explain the phenomenon.[4,5] Other effects such as lattice polarons due to Jahn−Teller (JT) distortion,[5] electron localization, and phase separation (PS) of carriers are advanced as an additional physics.[1] Charge ordering (CO) is a phenomenon observed in solids wherein electrons become localized due to the ordering of cations of differing charges on specific lattice sites. The charge-ordered phases are novel manifestations arising from the interaction between the charge carriers and the phonons wherein the JT distortions play a significant role.[6]

Among various options of cations entering the perovskite manganites, the Y and Ca types represent extreme cases due to their small size, resulting in a large tilt of the MnO_6 octahedra. In $R_{1-x}A_xMnO_3$, small R and A ions stabilize the charge-ordered state. A number of studies have shown that $x = 0.5$ compounds with small R and A ions exhibit two distinct transitions on cooling: a CO transition and a paramagnetic antiferromagnetic transition afterwards.[7,8] For $Y_{0.5}Ca_{0.5}MnO_3$ (YCMO), as the temperature decreases, the system first undergoes a transition to a CO state at $T_{CO} = 275$ K and then to a CE-type antiferromagnetic insulating state at $T_N = 125$ K.[8−12] Properties of selected YCMO compounds have been investigated widely.[8−12] However, Mössbauer data on the CO and magnetic transitions for Fe-doped YCMO are still missing.

In manganese perovskites $R_{1-x}A_xMnO_3$, Mössbauer spectroscopy (MS) in Fe-doped samples has contributed useful information.[14−18] The substitution with Fe has the advantage that it does not cause lattice distortion, because the Fe ion has an ionic radius the same size as that of the Mn ions. After ensuring that the doping (10%) of Fe at the Mn site of YCMO does not change the structure or the phase transition significantly,[19] we have carried out ^{57}Fe Mössbauer studies as a function of temperature from 293 to 80 K.

In this work, we have investigated the typical scenario of CO, JT distortions,[5] charge transfer,[20] and PS[1] in Fe-doped YCMO by MS, which is a local probe. To our best knowledge, it is the first that the dynamic isomer shift has been observed in Mössbauer spectra for Fe-doped YCMO. Furthermore, the microscopic method of MS has been used to identify two different Mn ions as Mn^{3+} and Mn^{4+} ions in the CO phase, appearing below T_{CO}, which has not been reported before for YCMO.

The Fe (10%)-doped $Y_{0.5}Ca_{0.5}MnO_3$ polycrystalline samples used in this work were prepared by the standard solid-state reaction of stoichiometric quantities of Y_2O_3, $CaCO_3$, MnO_2, and Fe_2O_3 (99.99 enriched), as described in ref 21. The phase purity was tested by X-ray diffraction patterns. Magnetization and magnetic susceptibility were measured with superconducting quantum interference device magnetometer (Quantum Design SQUID) in the range 4−300 K, and the data were taken at different applied fields and in the field-cooled (FC) and zero-field-cooled (ZFC) modes, respectively. The ^{57}Fe MS in transmission geometry was collected with a ^{57}Co γ-ray source, while the absorber was kept fixed in a variable-temperature cryostat. Velocity calibration was performed with the data of α-Fe at room temperature.

The X-ray diffraction analysis for the Fe-doped sample shows a single-phase perovskite structure, and the diffraction pattern could be indexed on an orthorhombic cell with $a = 0.535$ nm, $b = 0.541$ nm, and $c = 0.748$ nm. The structure is therefore

* To whom correspondence should be addressed. Tel/Fax: +86-431-5168246. E-mail: wtzheng@jlu.edu.cn.

10.1021/jp0444823 CCC: $30.25

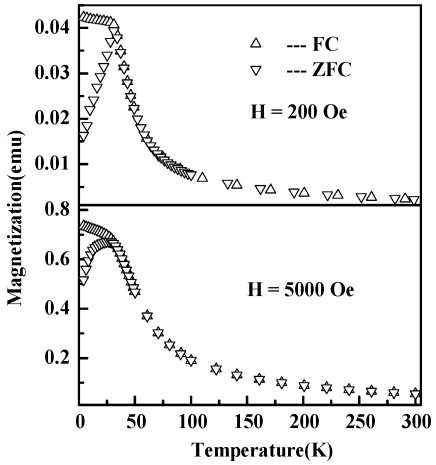

Figure 1. Temperature variation of the magnetization (FC and ZFC) of Fe-doped $Y_{0.5}Ca_{0.5}MnO_3$ at two different measuring fields.

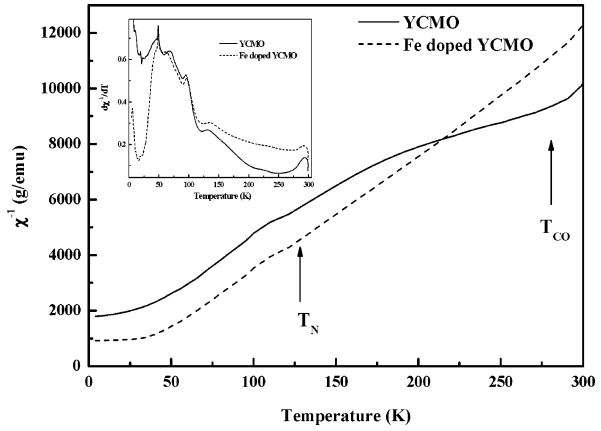

Figure 2. Temperature variation of the reciprocal of the magnetic susceptibilities of the Fe-doped YCMO sample and YCMO, respectively. The inset shows the derivative $d(\chi^{-1})/dT$.

the typical O′ type with $c/\sqrt{2} < a < b$, which is consistent with the parent compound YCMO.[8,9] FC and ZFC magnetizations obtained using fields of 200 and 5000 Oe are shown in Figure 1a−b. The branching temperatures are found to be 32 and 28 K, respectively. The Fe-doped sample shows the same magnetic behavior as its parent compound YCMO.[8,9] In Figure 2, we exhibit the reciprocal of the magnetic susceptibility (χ^{-1}) of the Fe-doped sample as a function of temperature. For comparison, the χ^{-1} of YCMO is also showed in the figure. In Figure 2, χ increases as T is lowered, but there is no sign of a sharp magnetic transition. One can easily see that the slope changes obviously in the $\chi^{-1}-T$ curve for the YCMO sample, and these changes denote the magnetic and CO transition temperatures.[7,8] To see the slope changes of the Fe-doped sample clearly, the $d(\chi^{-1})/dT$ curve is shown in the inset of Figure 2. Two derivative curves show the same varieties at the transition temperature. The antiferromagnetic and CO transition temperatures of Fe-doped sample can be derived in Figure 2: $T_N \approx 125$ K and $T_{CO} \approx 275$ K, which is consistent with its parent compound YCMO.[8,9,19]

The Mössbauer spectra as a function of temperature for the Fe-doped sample are shown in Figure 3, and the corresponding experimental data are listed in Table 1. The room-temperature spectrum is a single paramagnetic doublet with a central shift (δ_{CS}) of 0.349 ± 0.005 mm/s and a quadrupole splitting (Δ) of 0.372 ± 0.005 mm/s. The spectra retain the doublet character down to 80 K. The δ_{CS} is a typical value of high-spin Fe^{3+} (i.e., an S state with $S = 5/2$) with octahedral coordination. On

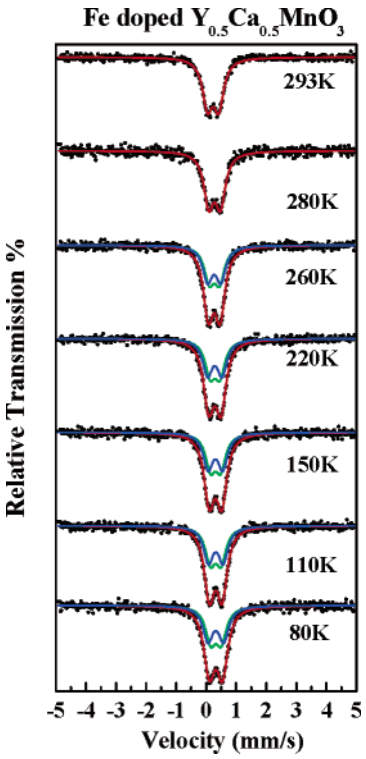

Figure 3. Mössbauer spectra of Fe-doped $Y_{0.5}Ca_{0.5}MnO_3$ in the 80−295 K range.

TABLE 1: Mössbauer Spectra Data of Fe-Doped $Y_{0.5}Ca_{0.5}MnO_3$ Sample

	central shift (δ_{CS})	quadrupole splitting (mm/s ± 0.005)		relative intensity (% ± 1)	
T (K)	(mm/s ± 0.005)	Δ1	Δ2	I1	I2
293	0.349	0.372		100	
280	0.397	0.386		100	
260	0.403	0.303	0.471	48.1	51.9
240	0.413	0.308	0.475	48.1	51.9
220	0.422	0.302	0.496	48.1	51.9
192	0.427	0.308	0.505	49.7	50.3
172	0.429	0.303	0.505	48.4	51.6
150	0.443	0.308	0.506	48.2	51.8
130	0.450	0.324	0.520	48.5	51.5
110	0.456	0.329	0.527	48.3	51.7
96	0.456	0.332	0.529	49.1	50.9
80	0.456	0.332	0.531	47.7	52.3

cooling the sample, δ_{CS} increases gradually and tends to saturate below 110 K, as can be seen in Figure 4a. The δ_{CS} is 0.349 mm/s at room temperature and increases to 0.413 mm/s at 240 K. After that, it remains nearly constant down to ~160 K and again increases significantly to 0.456 mm/s at 110 K. It seems that the δ_{CS} changes may be related to the CO transition and large distortion occurring at the two different temperatures. A very interesting phenomenon can be observed in Figure 4a. The inset of Figure 4a shows the variation of the lattice distortion index D of the YCMO sample with temperature.[8] As can be seen, the temperature-dependence behavior of δ_{CS} shows a tremendous similarity with D. This similarity cannot be a coincidence. To explain this similarity, the physics of the thermal shift (δ_T), which is temperature-dependent, has to be revealed.

Generally, the central shift (δ_{CS}) of the Mössbauer spectra should be the sum of the well-known isomer shift (δ) and the second-order Doppler shift (δ_{SOD}), that is

$$\delta_{CS} = \delta + \delta_{SOD} \quad (1)$$

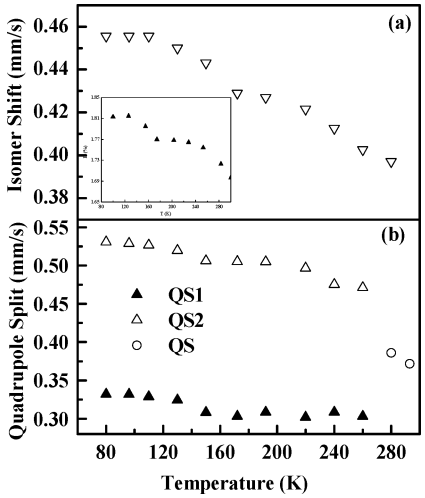

Figure 4. Temperature variation of (a) the isomer shift and (b) quadrupole splitting of Fe-doped $Y_{0.5}Ca_{0.5}MnO_3$. The inset in (a) is the variation of the lattice distortion index D of YCMO sample with temperature, which is taken from ref 12. In (b), the higher quadrupole splitting is designated $\Delta 2$ and the lower $\Delta 1$.

The first term arises from the coulomb interactions among the positively charged nuclei and electrons distributed around the nuclear site, and it is temperature-independent. The second term δ_{SOD} varies linearly with the mean-square velocity of the Fe^{57} nucleus and consequently shows a linear behavior with the temperature. Vanitha et al.[18] pointed out that the change in δ_{CS} with temperature is as expected from the relativistic second-order Doppler shift. If this is the case, the thermal shift will only be reflected in δ_{SOD}. Thus, the δ_{CS} value should show a linear behavior with the temperature, which is contrary to our experimental results. Shrivastava[24] proposed that the phonons in a lattice change the electron density at the site of the resonant nucleus, thereby causing a change in δ_{CS}. This change in δ_{CS} is highly temperature-dependent and is significantly smaller than the well-known isomer shift (δ). Hence, the dynamic isomer shift (δ_{DY}) must be included in total δ_{CS}, and the central shift can be rewritten as

$$\delta_{CS} = \delta + \delta_{SOD} + \delta_{DY} \quad (2)$$

The third term, δ_{DY}, arises from the interaction between electron and phonon, and it increases with decreasing temperature.[24] In eq 2, only the last two terms in δ_{CS} are temperature-dependent, that is to say, δ_T can be written as

$$\delta_T = \delta_{SOD} + \delta_{DY} \quad (3)$$

Because δ_{SOD} varies linearly with temperature, the origin of which has been discussed clearly, it will not be considered further. Only the temperature dependence of δ_{DY} will be concentrated on. It is well-known that the JT distortion is very strong in manganites, which can lead to a very strong electron−phonon coupling. Therefore, the temperature behavior of δ_{DY} can reflect the JT distortion to some extent. The significant increase in δ_{CS} at 160 K in Figure 4 may be related to the large distortion occurring in the YCMO sample at this temperature.[8] For the YCMO sample, using the extended X-ray absorption fine structure (EXAFS) technique, Gopalan and Kulkarni[10] have found that the value of the Debye−Waller factor with temperature is $\sim$0.001 Å^2 in the entire temperature range except for a marked increase by a factor of 2 in the region around 160 K. This marked increase is attributed to the large lattice distortions around 160 K. We believe that these lattice distortions around 160 K have considerable effect on the δ_{DY} measured by the MS, which leads to the observation that δ_{CS} does not vary linearly with temperature. Hence, using MS can detect the lattice distortion and give the same information as X-ray absorption technology.

What is the possible origin of δ_{DY}? Two possible reasons should be taken into account: (i) In the YCMO compound, as temperature is decreased, the *c* parameter contracts more prominently compared to the *a* and *b* parameters. The change in the *a* and *b* parameters in the temperature range of $T_N - T_{CO}$ is <1%, but the *c* parameter changes by about −8%.[8] This large contraction in the *c* parameter introduces a large orthorhombic distortion, which gives the strong cooperative JT distortion. As for our Fe-doped sample, the large contraction in the *c* parameter introduces a large distortion in FeO_6 octahedra, which may give an overlap of the 2p oxygen and 4s iron orbitals. The overlap increases as temperature decreases, which leads to an increase in s electron density at the iron nucleus, and δ_{DY} increases as a consequence. This orbital overlap may be attributed to 2p oxygen and 4s iron charge-transfer transitions in the FeO_6^{9-} octahedra. The similar overlap of 2p oxygen and 3d manganese charge-transfer transitions has been found in MnO_6^{9-} octahedra.[21] (ii) The other possible reason may have arisen from the strong crystal splitting in Fe-doped YCMO. The electronic configuration of Fe^{3+} is $3d^5$. The crystal field energy may promote an electron hopping from occupied $3d^5$ to an empty 4s orbital, thereby causing a change in the electron density at the site of the resonant nucleus. Hence, the dynamic isomer shift varies as s electron density changes.

From the Mössbauer experiment alone, one cannot separate the second-order Doppler shift δ_{SOD} from the dynamic isomer shift δ_{DY}. [24] However, our experimental data show that the electron−phonon interaction plays a very important role in explaining the temperature-dependent δ_{CS}.

The temperature variations of Δ in Fe-doped YCMO have been shown in Figure 4b. The Δ value increases with decreasing temperature, showing a jump around 270 K (T_{CO}). This abrupt change in Δ below T_{CO} can be related to the CO transition.[16−18] Below 280 K, to obtain a correct spectrum analysis, we have to introduce a second Fe^{3+} doublet whose central isomer shift has the same value as the first one, but the quadrupole splitting Δ is different. The fitted Mössbauer spectra are shown in Figure 3. The two contributions in Figure 3 have about equal intensities ($\sim$50%, see Table 1). The quadrupole splitting determined by Mössbauer spectra, plotted in Figure 4b, shows two components below 280 K, one with a higher Δ value ($\Delta 2$) and the other with a lower Δ value ($\Delta 1$) than that of the room-temperature spectrum. A similar behavior has been reported from a study of the MS of the CO $Sm_{0.5}Ca_{0.5}Mn_{0.985}Fe_{0.015}O_3$ and $Nd_{0.5}Ca_{0.5}Mn_{0.98}Fe_{0.02}O_3$ below the CO temperature.[17,18] There is a slight difference between the line width of Mn^{4+} and line width of Mn^{3+} (not shown), and these two components are almost kept constant ($\sim$0.20 mm/s) in the temperature range of T_{CO} (275 K) and T_N (125 K). The almost constant and small value of line width indicates that all of the Mn^{3+} (Mn^{4+}) ions see the same electric field gradient. A narrow distribution of Mn^{3+} gradients (Mn^{4+} gradients) suggests that the charge ordering is complete in this temperature range.

The two Fe^{3+} doublets in Figure 3 indicate that there exist two different Mössbauer sites in Fe-doped YCMO, and the two doublets can be explained by the location of the Fe^{3+} ions in two different manganese sites, created by the CO between Mn^{3+} and Mn^{4+}. The two different manganese sites in CE-type antiferromagnetic CO manganite are explained well by the

model proposed by Goodenough.[22] In his model, Mn^{3+} and Mn^{4+} are interlaced like a checkerboard (see Figure 1, ref 23) and the Mn^{3+} sites have a strong JT distortion; hence, the CO manganites consist of a mixture of strong JT-distorted and little-distorted MnO_6 octahedra. It should be emphasized that the so-called CO is characterized by the presence of two different types of Mn atom with different local geometrical structures in manganites. This fact implies that the total charge on each type of Mn atom should be different, and the charge density should show spatial anisotropy induced by the local geometrical structure. When Fe is doped into YCMO, Mn^{3+} and Mn^{4+} will be substituted by iron, which can be revealed in detail by the Mössbauer experiment. The doublet characters in the Mössbauer spectra are due to a nonzero electric gradient at the iron site,[16] and a bigger electric gradient leads to a higher Δ value. The different Δ values at two different iron sites indicate that the local geometrical structures of Mn^{3+} and Mn^{4+} ions were originally different. Thus, we can deduce that $\Delta 2$ and $\Delta 1$ represent the original Mn^{3+} and Mn^{4+} sites, respectively.

The identification of two different Mn ions has been performed by means of neutron diffraction and electron microscopy.[3,13] In the latter case, the electronic image shows stripes with a periodic ordering that has been described as being caused by the ordering of Mn^{3+} and Mn^{4+} ions.[13] Needless to say, there is solid proof of the existence of two different Mn ions in the CO phase, but neither neutron diffraction nor electronic microscopy can confirm the identification of these as Mn^{3+} and Mn^{4+} ions. However, MS can be used to distinguish between the Mn^{3+} and Mn^{4+} ions in CO manganites, which is an advantage over other techniques.

In Figure 4b, $\Delta 1$ and $\Delta 2$ increase as the temperature decreases. The main cause of the change in both Δ should be the gradual deformation of the MnO_6 octahedra with the development of the JT distortion.[11] Furthermore, both $\Delta 1$ and $\Delta 2$ become constant below 110 K, which is possibly because charge ordering and the structural change are both complete around this temperature.[11,18]

In summary, we report the MS study on Fe-doped CO manganite YCMO. The changes in the central isomer shift and quadrupole splitting of MS as a function of temperature are investigated to understand the hyperfine properties in this system. The dynamic isomer shift is observed for CO manganite, and its origin may be related to the electron transfer from the 2p oxygen and 4s iron orbitals or the electron hopping from Fe^{3+} occupied $3d^5$ to an empty 4s orbital. The MS spectra for Fe-doped YCMO can be interpreted in terms of two doublets arising because of the presence of two different Mn sites below the charge-ordering temperature. This confirms that there exist two different Mn ions (i.e., Mn^{3+} and Mn^{4+} ions), which can be identified by the microscopic method of Mössbauer spectroscopy.

References and Notes

(1) Dagotto, E.; Hotta, T.; Moreo, A. *Phys. Rep.* **2001**, *344*, 1.

(2) Jin, S.; Tiefel, T. H.; McCormack, M.; Fastnacht, R. A.; Ramesh, R.; Chen, L. H. *Science* **1994**, *264*, 413.

(3) Radaelli, P. G.; Marezio, M.; Hwang, H. Y.; Cheong, S.-W.; Batlogg, B. *Phys. Rev. Lett.* **1995**, *75*, 4488.

(4) Zener, C. *Phys. Rev.* **1951**, *81*, 440.

(5) Millis, A. J.; Littlewood, P. B.; Shraiman, B. I. *Phys. Rev. Lett.* **1995**, *74*, 5144.

(6) Rao, C. N. R.; Arulraj, A.; Cheetham, A. K.; Raveau, B. *J. Phys.: Condens. Matter* **2000**, *12*, R83.

(7) Blasco, J.; Garcia, J.; de Teresa, J. M.; Ibarra, M. R.; Perez, J.; Algarabel, P. A.; Marquina, C.; Ritter, C. *J. Phys.: Condens. Matter* **1997**, *9*, 10321.

(8) Arulraj, A.; Gundakaram, R.; Biswas, A.; Gayathri, N.; Raychaudhuri, A. K.; Rao, C. N. R. *J. Phys.: Condens. Matter* **1998**, *10*, 4447.

(9) Tian, H. W.; Zheng, W. T.; Zhao, Z. D.; Ding, T.; Yu, S. S.; Zheng, B.; Li, X. T.; Jiang, Q. *Chem. Phys. Lett.* **2005**, *401*, 585.

(10) Srinivasa Gopalan, R.; Kulkarni, G. U. *Solid State Commun.* **1998**, *105*, 371.

(11) Causa, M. T.; Aliaga, H.; Vega, D.; Tovar, M.; Alascio, B.; Salva, H. R.; Winkler, E. *J. Magn. Magn. Mater.* **2004**, *272*−*276*, 81.

(12) Dlouha, M.; Vratislav, S.; Jirak, Z.; Hejtmanek, J.; Knizek, K.; Sedmidubsky, D. *Appl. Phys. A* **2002**, *74*, S673.

(13) Chen, C. H.; Cheong, S.-W. *Phys. Rev. Lett.* **1996**, *76*, 4042.

(14) Chechersky, V.; Nath, A.; Isaac, I.; Franck, J. P.; Ghosh, K.; Greene, R. L. *Phys. Rev. B* **2001**, *63*, 052411.

(15) Cheng, Z. H.; Wang, Z. H.; Di, N. l.; Kou, Z. Q.; Wang, G. J.; Li, R. W.; Lu, Y.; Li, Q. A.; Shen, B. G.; Dunlap, R. A. *Appl. Phys. Lett.* **2003**, *83*, 1587.

(16) Kallias, G.; Pissas, M.; Devlin, E.; Simopoulos, A. *Phys. Rev. B* **2002**, *65*, 144426.

(17) Studer, F.; Nguyen, N.; Toulemonde, O.; Ducouret, A. *Int. J. Inorg. Mater.* **2000**, *2*, 671.

(18) Vanitha, P. V.; Nagarajan, R.; Rao C. N. R. *J. Solid State Chem.* **2003**, *174*, 74.

(19) Vanitha, P. V.; Singh, R. S.; Natarajan, S.; Rao C. N. R. *Solid State Commun.* **1999**, *109*, 135.

(20) Moskvin, A. S. *Phys. Rev. B* **2002**, *65*, 205113.

(21) Ding, T.; Zheng, W. T.; Tian, H. W.; Zang, J. F.; Zhao, Z. D.; Yu, S. S.; Li, X. T.; Meng, F. L.; Wang, Y. M.; Kong, X. G. *Solid State Commun.* **2004**, *132*, 815.

(22) Goodenough, J. B. *Phys. Rev.* **1955**, *100*, 564.

(23) Mizokawa, T.; Fujimori, A. *Phys. Rev. B* **1997**, *56*, R493.

(24) (a) Shrivastava, K. N. *Phys. Rev. B* **1970**, *1*, 955. (b) Shrivastava, K. N. *Phys. Rev. B* **1973**, *7*, 921.